

Bifurcated States of Ohmically Heated Tokamak Plasmas

M. R. de Baar, G. M. D. Hogeweij, and N. J. Lopes Cardozo

*FOM Instituut voor Plasmafysica "Rijnhuizen," Association EURATOM-FOM, Trilateral Euregio Cluster, P.O.Box 1207,
3430 BE Nieuwegein, The Netherlands*

(Received 24 April 1998; revised manuscript received 17 September 1998)

Experiments in the Rijnhuizen Tokamak Project are reported which show bifurcated states of plasmas in the linear Ohmic confinement regime. One branch is the usual Ohmic state. The second, newly discovered, state features a much broader temperature profile, while the density has a very pronounced gradient near the half radius. The bifurcated states form after off-axis electron cyclotron heating is switched off. The new state contradicts theoretical models which predict improved confinement for peaked density profiles or high collisionality. [S0031-9007(98)08046-6]

PACS numbers: 52.55.Fa, 52.25.Fi, 52.50.Gj

In tokamaks [1], hot plasmas are confined in a torus by means of an externally applied toroidal magnetic field (B_ϕ) and a much smaller poloidal field, which result from a toroidal current density j . The plasma torus is characterized by the major radius (R_0) and the minor radius (a). The helical field lines lie on nested tori, with minor radius r , or $\rho = r/a$. The safety factor (q), defined as the number of toroidal turns a field line makes to complete one poloidal turn, is a function of ρ .

For tokamak discharges without additional heating, the energy confinement time τ_E is proportional to n_e [linear Ohmic confinement (LOC)] at low electron density (n_e), while above a line-average density of $\bar{n}_{e,cr} = 3-5 \times 10^{19} \text{ m}^{-3}$ confinement becomes independent of n_e [saturated Ohmic confinement (SOC)]. It has been shown in many tokamaks [2-5] that SOC is due to saturation of the electron energy content W_e . By forcing the density profile to peak it is possible to go from SOC to improved Ohmic confinement (IOC), where the linear scaling of τ_E with n_e is recovered. Statistical analysis indicates that IOC is a high density continuation of LOC [3]. In the three regimes the q profile reaches just below unity in the center of the discharge.

The n_e dependence of τ_E is often brought into relation to the density peakedness, $Q_n = n_e(0)/n_e^v$, in which n_e^v is the volume-average density. It has been observed that in LOC, Q_n increases with n_e , that Q_n is constant or even slightly decreasing in SOC, and increases again in IOC. Q_n is associated with the density gradient length $L_n = n_e/\nabla n_e$ and can be increased actively by multiple pellet injection [6,7] or reduction of the edge density by tailoring the edge-radiation profile with low Z_{eff} impurities [8]. Several scenarios for turbulent transport have been put forward in the literature to explain the complicated dependence of τ_E on Q_n . The candidate modes [the dissipative trapped ion mode (DTIM), the dissipative trapped electron mode (DTEM), the ion temperature gradient mode (ITGM or η_i mode), and electron temperature gradient mode (ETGM or η_e mode)] are either stabilized with decreasing L_n [9,10] or increasing collisionality ν .

The present paper reports on the Rijnhuizen Tokamak Project (RTP) ($R_0 = 0.72 \text{ m}$, $a = 0.16 \text{ m}$, $B_\phi < 2.5 \text{ T}$, pulse length typically 0.5 s discharges which are all in the LOC regime. Two distinct Ohmic states have been observed. One is the normal Ohmic state with a peaked T_e profile and central q touching unity. The second, newly found, state has a much broader T_e profile, a q profile which stays well above unity, and high- Q_n n_e profile, with strong local gradients near the half radius.

The plasma was heated at half radius with 350 kW, 110 GHz electron cyclotron heating (ECH) (second harmonic, X mode, launched from the low field side) during 150 ms, corresponding to >30 energy confinement times and >5 current diffusion times. The ECH power exceeds the Ohmic dissipation by a factor >5 . When the ECH deposition is placed off axis, in RTP the steady state flat or hollow T_e profiles are obtained [11]. This contrasts the finding in DIII-D, where off-axis ECH led to peaked T_e profiles [12]. However, both experiments have in common the fact that significant heat convection up the T_e gradient must be invoked to explain the power balance. Importantly, in the off-axis heated RTP plasmas, the central q is increased well above $q = 2$, and a region with small or inverted shear is created. When this state is allowed to relax by switching off the ECH, the two stable Ohmic states can be accessed.

We consider a database of 37 RTP discharges with very similar parameters ($B_\phi = 2.26 \text{ T}$, $I_p = 80 \text{ kA}$, and $\bar{n}_e = 3 \times 10^{19} \text{ m}^{-3}$), with $\rho_{\text{dep}} = 0.55$. Figure 1 shows the evolution of $T_e(0)$ measured with electron cyclotron emission spectroscopy (ECE) (top panel) and n_e as measured with an interferometer (bottom panel) in two typical discharges. Note that $T_e(0)$ decreases during off-axis ECH, when a hollow T_e profile develops. The discharges reach almost the same steady state during the ECH, but evolve differently after ECH is switched off. State-I discharges (red) feature values for $T_e(0)$ and Q_n that are similar to the pre-ECH phase, while state-II discharges (green) feature lower $T_e(0)$ and higher Q_n . The two branches reach a steady state and remain separated until the end of

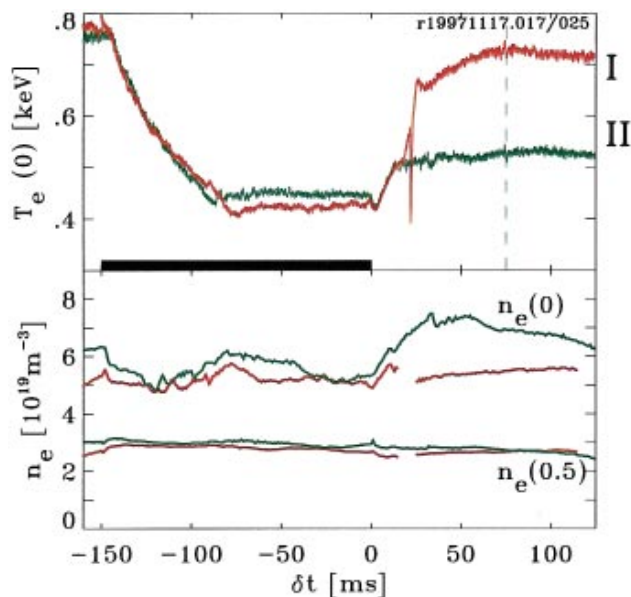


FIG. 1(color). The evolution of the central electron temperature $T_e(0)$ (top panel) for two representative discharges, which have near identical parameters. During the off-axis ECH ($\delta t = [-150, 0]$ ms), the profiles of T_e and j become hollow, hence $T_e(0)$ decreases. After switch off of the ECH, two distinct branches form. The state-I discharge (red) returns to a state that is very similar to the pre-ECH Ohmic plasma. The state-II discharge (green) settles at a much lower $T_e(0)$. The bottom panel shows the behavior of the central density and the density at half radius. After switch off of the ECH, the state-II n_e profile becomes more peaked. The state-I discharge passes through a few instabilities (see Fig. 6), which distort the interferometer signals for a short period. The profiles of both states, measured with Thomson scattering at $\delta t = 75$ ms (indicated by the dashed line), are compared in Fig. 4.

the discharge, i.e., >30 energy confinement times and >5 current diffusion times. The database shows that there are indeed distinct branches, separated by a gap (Fig. 2).

Figure 3 compares the profiles of T_e , n_e , and electron pressure (p_e) in the two branches, measured with multi-position Thomson scattering 75 ms after ECH has been switched off, i.e., well into the steady state phase. The high T_e -branch (state-I, red) and the low T_e -branch (state-II, green) profiles are similar in the outer region ($\rho > 0.4$), but diverge in the center. State-I is very similar to the pre-ECH state of the discharge albeit that the central T_e is often (but not always) slightly lower. The n_e and T_e profiles are triangular. The state-II n_e profiles develop a steep gradient at $\rho \approx 0.38$. Note that no pellet injection was applied. State-II has less peaked pressure profiles than state-I. The Ohmic dissipation is 130 and 165 kW for the state-I and state-II discharges presented here.

The fact that both states are in LOC has been established experimentally. In Fig. 4 the T_e and n_e profiles are presented for discharges with different \bar{n}_e . The variation in density is 13% for the state-II discharges and 20% for the state-I discharges. The T_e profiles are very similar and show no density dependence. The density profiles

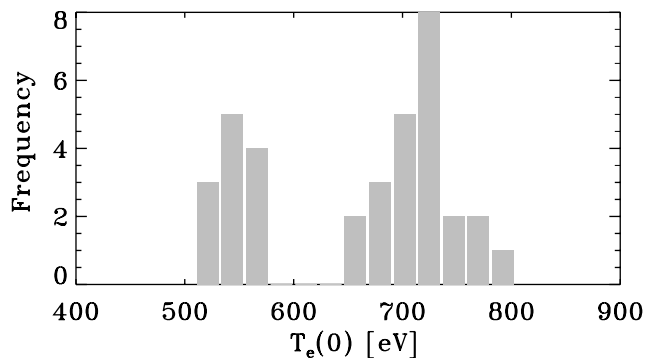


FIG. 2. A histogram of the steady state central electron temperature, reached 75 ms after ECH is switched off, of 37 near identical discharges. The gap between state-I and state-II is clearly observed. Detailed analysis shows that state-I may in fact consist of two distinct states, the upper one of which corresponds to the pre-ECH Ohmic state.

are self-similar. $Q_n = 3.04$ and 3.11 for the low and high density state-II discharges, respectively. $Q_n = 2.82$ and 2.78 for the low and high density state-I discharges, respectively. For both states, W_e and τ_E increase linearly with density. This result agrees with the density at which saturation is expected for $I_p = 80$ kA RTP discharges,

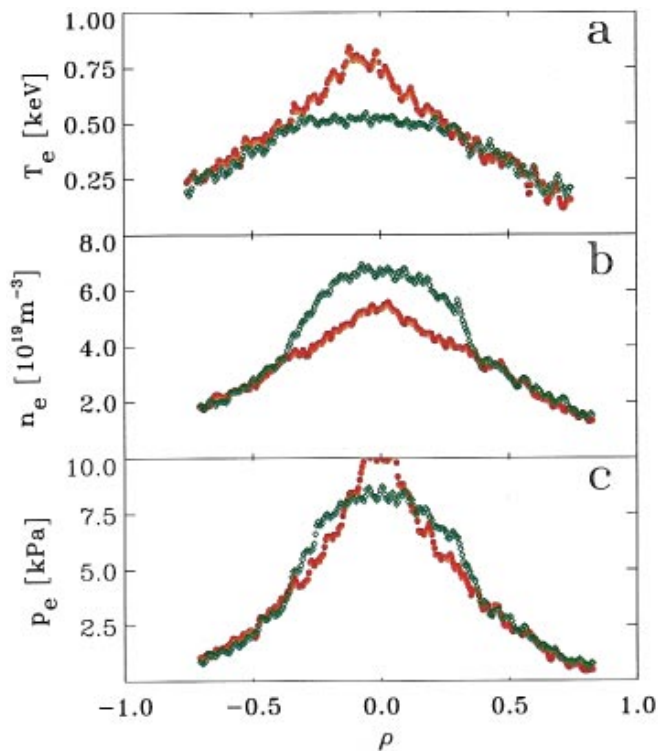


FIG. 3(color). Profiles of (a) T_e , (b) n_e , and (c) p_e measured with Thomson scattering at 75 ms into the post-ECH phase for both states (red: state-I, green: state-II). In state-II the n_e profile develops a localized gradient near $\rho = 0.38$. The differences are very pronounced in the T_e and n_e profiles but largely cancel in the p_e profile, which nonetheless is more peaked in state-I than in state-II. For the presented discharges, $\tau_E^I = 4.4$ ms and $\tau_E^{II} = 4.2$ ms.

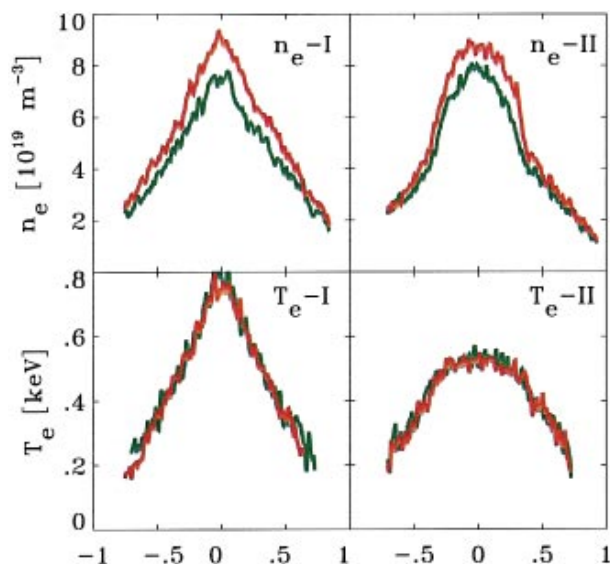


FIG. 4(color). T_e and n_e profiles for the two states at different densities (high n_e in red, low n_e in green). For both states, the increase of n_e is not associated with changes in T_e . The profile shapes are constant, and $W_e \propto \bar{n}_e$.

$\bar{n}_{e,cr} = 4.3 \times 10^{19} \text{ m}^{-3}$. This is 30% higher than the highest density presented in this paper. State-I discharges follow the neo-Alcator scaling, and state-II discharges do 25% worse.

In Fig. 5 a sequence of T_e (a) and n_e profiles (b) is presented for discharges which evolve to state-II. When ECH is switched off, the off-axis maximum in T_e is not sustained and $T_e(\rho > \rho_{dep})$ decreases within the first

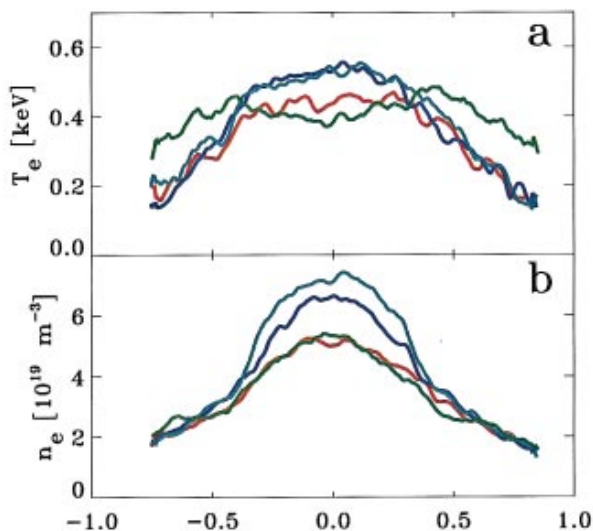


FIG. 5(color). Development of state-II profiles. The profiles shown are taken 0 ms (green), 3 ms (red), 20 ms (dark blue), and 35 ms (light blue) after ECH is switched off. The T_e profile changes rapidly after switch off, but is at 3 ms (i.e., about one energy confinement time) already close to its final state. The changes in the n_e profile, most notably the formation of a steep ∇n_e region around $\rho = 0.38$ take tens of ms, or several current diffusion times.

3 ms, while $T_e(0)$ increases slightly. The sharp n_e gradient around $\rho = 0.38$ develops on a much longer time scale. Why this local gradient forms is not clear. Influx of neutral particles can be ruled out as an explanation for the differences in the two states, because (1) the neutrals come from the edge region of the plasma where both states are similar and (2) a neutral influx cannot explain such a localized increase of ∇n_e . Specific effects of ECH, such as anisotropy or deformation of the velocity distribution function, should disappear much faster than the gradual buildup of the density gradient. The gradient formation must then be due to a reduction of the local particle diffusion coefficient, an increase of the inward particle convection or a combination of the two effects. So far we are not able to distinguish between these effects, and the question as to why the steep n_e gradient forms remains open.

With the high Q_n and the linear τ_E dependence on \bar{n}_e , state-II profiles may appear to be a low density variant of IOC discharges. However, we note the following essential differences: (1) The bifurcation of the T_e profile is already established long before the n_e profile peaks; (2) the state-II discharges have worse (rather than “improved”) confinement compared to state-I; (3) the state-II discharges develop a n_e gradient, which is much more localized than the profile peaking reported for IOC discharges. Moreover, in state-II discharges, the n_e peaking is not the consequence of density profile control but evolves spontaneously. Finally, the state-II is produced at much lower density than IOC.

Figure 6 depicts traces of T_e , measured by ECE, showing two fast relaxations that occur only in state-I discharges. The first event is localized off axis, and often displays precursor activity with an $m = 2, n = 1$ character, as could be determined from ECE and soft x-ray measurements. Off-axis relaxation phenomena with $m \neq 1$ are observed in many tokamaks [13–15] and are often associated with nonmonotonical q profiles. The second, more violent, event also affects the center of the discharge. The steep n_e gradient near $\rho = 0.38$ disappears within 1 ms after this event. For this event, precursor activity has not been observed.

In equilibrium, the current density $j(\rho)$ (see Fig. 7a) can be calculated from T_e and p_e assuming neoclassical resistivity. In leading order, the bootstrap current is driven by ∇n_e and the effect of the steep ∇n_e region for state-II discharges is clearly visible. The effect of the bootstrap current is that, in addition to the effect of the flat T_e region, the q profile (see Fig. 7c) remains flat out to $\rho = 0.38$ for state-II discharges with $q_{min} \approx 1.8$. For state-I discharges $q_{min} \approx 1$. The observation that the two branches separate when an $m = 2$ MHD event occurs, after which the two branches have very different q profiles, may indicate a role of the q profile in the transport physics.

In conclusion, a new Ohmic state has been found, in which the energy confinement is proportional to the density as in normal LOC discharges. In this state a sharp

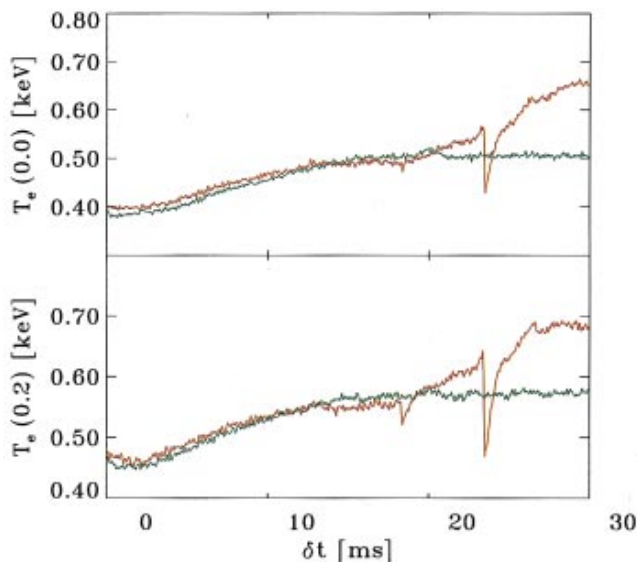


FIG. 6(color). ECE measurements of the electron temperature at $\rho = 0$ and $\rho = 0.2$, showing two “fast events” in a state-I discharge (red). State-II traces (green) are also presented. The first event coincides with the divergence of the two states, and may be the cause of it. This event does not affect the center, and often has an $m = 2$ precursor. The second event is much stronger and does affect the center.

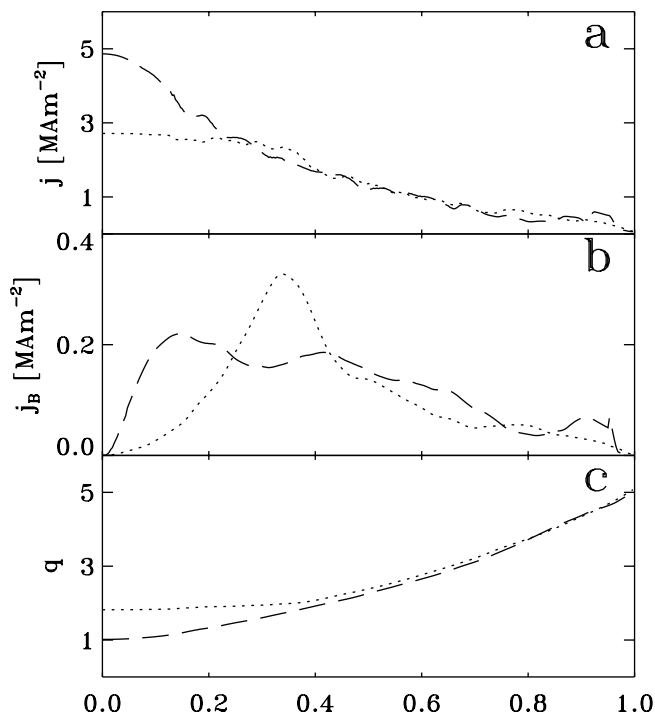


FIG. 7. Profiles of the total current density $j(\rho)$ (a), bootstrap-current profile $j(\rho)_B$ (b), and the safety factor $q(\rho)$ (c) for both states (state-I: dashed line; state-II: dotted line). The effect of the off-axis maximum of the bootstrap current for state-II discharges is that $j(\rho)$ and $q(\rho)$ remain flat from the center up to $\rho = 0.38$.

n_e gradient forms spontaneously near $\rho = 0.38$. In theoretical models commonly forwarded to explain the LOC-SOC and IOC regimes, it is thought that density peaking or increased collisionality leads to improved confinement. In contrast, in the present experiment the density peaking arises spontaneously, comes after the bifurcation, and does not lead to improved confinement. Since both state-I and state-II are in the LOC regime, and state-I follows the usual neo-Alcator scaling, the coexistence of both states appears to be at variance with the usual picture in which turbulent modes which are sensitive to L_n or ν are responsible for transport. Furthermore, from the steady state profiles and the evolution of state-II, it is evident that χ_e and D are decoupled, thus differing from the conclusion reached in Ref. [5] for LOC discharges. As an alternative, the present experiments indicate a role of the q profile determining the transport of heat and particles. This places the present results in a wider class of experiments with intense additional heating or pellet injection, where an extreme sensitivity of confinement to initial conditions was found, which was related to the evolution of the q profile [15–20]. Thus, the bifurcation of Ohmic plasma states reported here, and, e.g., the formation of an electron transport barrier in JET discharges with “optimized shear” [19], may have a common physical explanation.

We thank Dr. F. C. Schüller and Dr. A. A. M. Oomens for stimulating discussion, and the RTP team for machine and diagnostic operation. This work was done under the Euratom-FOM Association agreement with financial support from NWO and Euratom.

- [1] J. A. Wesson, *Tokamaks* (Clarendon Press, Oxford, 1997), p. 12–13.
- [2] X. Garbet *et al.*, Nucl. Fusion **32**, 2147–2155 (1992).
- [3] E. E. Simmet *et al.*, Plasma Phys. Control. Fusion **38**, 689–704 (1996).
- [4] F. Alladio *et al.*, Plasma Phys. Controlled Nucl. Fusion Res. **1**, 153 (1991).
- [5] G. Becker, Nucl. Fusion **30**, 2285–2193 (1990).
- [6] M. Kaufmann *et al.*, Nucl. Fusion **28**, 827–848 (1988).
- [7] M. Greenwald *et al.*, Phys. Rev. Lett. **53**, 352 (1984).
- [8] M. Bessenrodt *et al.*, Nucl. Fusion **31**, 155 (1991).
- [9] F. Romanelli *et al.*, Nucl. Fusion **26**, 1515 (1986).
- [10] Y. C. Lee *et al.*, Phys. Fluids **30**, 1331 (1987).
- [11] G. M. D. Hogewij *et al.*, Phys. Rev. Lett. **76**, 632 (1996).
- [12] T. C. Luce, C. C. Petty, and J. C. M. de Haas, Phys. Rev. Lett. **68**, 52 (1992).
- [13] R. M. Meulenbroeks *et al.* (to be published).
- [14] Z. Chang *et al.*, Phys. Rev. Lett. **77**, 3553 (1996).
- [15] M. R. de Baar *et al.*, Phys. Rev. Lett. **78**, 4573 (1997).
- [16] P. Smeulders *et al.*, Nucl. Fusion **35**, 225–242 (1995).
- [17] N. J. Lopes Cardozo *et al.*, Plasma Phys. Control. Fusion **39**, B303–B316 (1997).
- [18] Y. Koide *et al.*, Phys. Rev. Lett. **72**, 3662 (1994).
- [19] A. C. C. Sips *et al.*, Plasma Phys. Control. Fusion **40**, 647–652 (1998).
- [20] R. E. Bell *et al.*, Plasma Phys. Control. Fusion **40**, 609–613 (1998).